

The Size of IDV Jet Cores

T. Beckert, T. P. Krichbaum, G. Cimò, L. Fuhrmann, A. Kraus,
A. Witzel, J. A. Zensus

Max-Planck-Institut für Radioastronomie,
Auf dem Hügel 69, 53121 Bonn, Germany
tbeckert@mpifr-bonn.mpg.de

Abstract

Radio variability on timescales from a few hours to several days in extragalactic flat-spectrum radio sources is generally classified as intra-day variability (IDV). The origin of this short term variability is still controversial and both extrinsic and intrinsic mechanisms must be considered and may both contribute to the observed variations. The measured linear and circular polarization of IDV sources constrains the low energy end of the electron population. Any population of cold electrons within sources at or above the equipartition temperature of 10^{11} K depolarizes the emission and can be ruled out. Intrinsic shock models are shown to either violate the large fraction of sources displaying IDV or they do not relax the light travel time argument for intrinsic variations. From structure function analysis, we further conclude that interstellar scintillation also leads to tight size estimates unless a very local cloud in the ISM is responsible for IDV.

Keywords: quasars: individual (0917+624)—ISM: structure—turbulence

1 Introduction

Intraday Variability (IDV) of flat-spectrum compact Quasar cores and BL Lacs at cm-wavelength has been discovered in 1985 (Heeschen et al., 1987) and is a common phenomenon ($\sim 25\%$) (Quirrenbach et al., 1992) among these sources. On rare occasions in 0716+714 and 0954+658, correlations with optical variations have been found and the evidence has been reviewed several times (e.g. Wagner S.J., Witzel A., 1995; Krichbaum, this volume). Radio-optical correlations, if real, suggest either fast intrinsic variations or gravitational lensing. From the light travel time argument the apparent brightness temperatures T_b are in the range of 10^{17} – 10^{21} K and far in excess of the intrinsic inverse Compton (IC) limit of 10^{12} K. The observed superluminal motions of jet components in many of these sources imply $\Gamma = 5$ – 10 and allow for Doppler boosting factors $\mathcal{D} = (\Gamma(1 - \beta \cos \theta))^{-1}$ and time shortening, which are insufficient for reducing the apparent T_b down to the IC limit. The required Doppler factors \mathcal{D} are

in the range of 60 up to 1000. Furthermore jets with a surface brightness at the IC limit are radiatively inefficient (Begelman, Rees & Sikora, 1994) and carry most of their energy as bulk motion. This is not supported by the observed power of radio lobes of these sources and raises the energy requirement for the central engine to an uncomfortable level. It is therefore argued (Readhead, 1994; Begelman, this volume) that incoherent synchrotron sources in jets should radiate at the equipartition temperature $T_E \approx 10^{11}$ K. This enforces Doppler factors which are 2–3 times larger than for the IC limit. Furthermore synchrotron sources at the IC limit with bulk motions of $\Gamma > 100$ are dominated by inverse Compton scattering of either AGN photons (Begelman, Rees & Sikora, 1994) or CMB photons at redshifts $z \sim 1$ and not by the SSC process. The cooling is catastrophic, independent of the brightness temperature, and this explanation must therefore be discarded.

Other more tempting suggestions are the propagation of relativistic thin shocks in the jets (Qian et al., 1991), so that the observed variability timescale is not a measure of the source size, and scintillation induced by the interstellar medium (e.g. Rickett 1990) of otherwise non-variable sources. We will explore both explanations in the following sections.

2 Cool Particle Depolarization

The emission of incoherent synchrotron sources with high brightness temperatures is dominated by radiation from the $\tau = 1$ surface. For intrinsic T_b 's above the equipartition temperature, the energy of the source is dominated by particles (e^- , e^+ , p) with a strong dependence on T_b :

$$U_e/U_B \propto T_b^{7+2\alpha} \quad ,$$

where α is the optically thin spectral index of the emission. Above the IC limit any contribution of cold electrons in an e^-/p plasma will depolarize the synchrotron emission. Emission from the $\tau = 1$ surfaces of flat spectrum radio cores comes predominantly from electrons with constant γ_{rad} -factor, independent of frequency. We consider power-law distributions of electrons $N(\gamma) \propto \gamma^{-p}$ above a lower cut-off γ_{min} . The degree of linear polarization is likely to be reduced by tangled magnetic fields in a turbulent plasma with a typical wavenumber k_0 in sources of size R (e.g. jet radius). For independent variations of magnetic field orientation in adjacent cells of size k_0^{-1} the fractional linear polarization is $\pi_L \propto (k_0 R)^{-3/2}$. Further depolarization inside one cell occurs, if Faraday rotation by electrons around γ_{min} (Jones & O'Dell 1977) depolarizes the radiation within the cell $\pi_L \propto \tau/\tau_F$. Here τ_F is the Faraday depth in the cell, which is smaller than the Faraday depth for the whole source by a factor $(k_0 R)^{-1}$. The fractional linear polarization can then be approximated by

$$\pi_L \approx \frac{\alpha + 1}{\alpha + 5/3} (k_0 R)^{-1/2} (\gamma_{\text{rad}}/\gamma_{\text{min}})^{-p} \frac{\gamma_{\text{min}}}{\ln \gamma_{\text{min}}} \quad . \quad (1)$$

For sources above the IC limit the magnetic field strength must be very low and radiation at GHz-frequencies is emitted by electrons with large γ_{rad} . The resulting ratio

$\gamma_{\text{rad}}/\gamma_{\text{min}}$ in Eq.1 becomes large, and the polarization drops below 1% if $\gamma_{\text{min}} < 10^3$ at $T_b = 10^{12}$ K. At the equipartition temperature we still have depolarization if $\gamma_{\text{min}} < 80$. The fact that most IDV sources are variable in polarized flux with a mean $\pi_L \geq 1\%$ requires a cut-off in the electron population close to γ , which dominates the radiation from $\tau = 1$ surfaces. At $T_b > 10^{13}$ K this requires fine-tuning of γ_{min} and provides strong constraints for acceleration mechanisms. Any substantial population of cold electrons with $\gamma_{\text{min}} \approx 1$ is excluded in polarized sources with $T_b > 10^{10}$ K. This problem does not arise in pair plasma jets, because Faraday depolarization does not occur there.

3 The alignment problem of thin shock propagation

The thickness Δz of a layer of post shock gas behind a relativistic shock, which travels with a shock-Lorentz-factor $\Gamma_S > 2$ for a distance z is

$$\Delta z = \left(1 - \sqrt{\frac{\Gamma_S^2 - 4}{\Gamma_S^2 - 1}} \right) z \quad , \quad (2)$$

assuming that the gas leaves the shock at the sound speed and has an ultra-relativistic equation of state. A gas element that passed through the shock at $z = 0$ is separated by a distance Δz from the shock, when the shock has travelled a distance z in the jet frame. For oblique shocks (as suggested by Spada et al., 1999) the velocity and the thickness of the post shock gas will be larger. The ratio of thickness to the square-root of the surface area is

$$\tilde{\tau} \approx \Delta z / (\sqrt{\pi} z \sin \psi) = \left(1 - \sqrt{\frac{\Gamma_S^2 - 4}{\Gamma_S^2 - 1}} \right) / (\sqrt{\pi} \sin \psi) \quad , \quad (3)$$

where it is assumed that the shock travelled at a constant velocity from the tip of a conical jet with half opening angle ψ . In the following we will assume that the shock travels only 1/10 of that distance. When the shock is viewed face on, the surface area is a factor $1/\tilde{\tau}^2$ larger than inferred from the variability timescale. But this factor is subject to relativistic aberration

$$\tau = \mathcal{D} \sin \theta + \Gamma \mathcal{D} \tilde{\tau} (\cos \theta - \beta) \quad , \quad (4)$$

where β is the velocity of the post-shock gas and θ the angle between jet and the line of sight. The true observed flux variations can arise from orientation changes of shock and jet

$$\frac{\Delta F_{\text{obs}}}{F_{\text{int}}} = f_1 = 3\mathcal{D}^2 \frac{\partial \mathcal{D}}{\partial \theta} \tau^{-2} \Delta \theta \quad , \quad (5)$$

or from inhomogeneities in particle density or magnetic field along the jet (Qian et al., 1991), which are scanned by the shock and travel with the sound speed through the post-shock gas

$$\frac{\Delta F_{\text{obs}}}{F_{\text{int}}} = f_2 = \mathcal{D}^3 (\tau/0.667)^{-2} \quad . \quad (6)$$

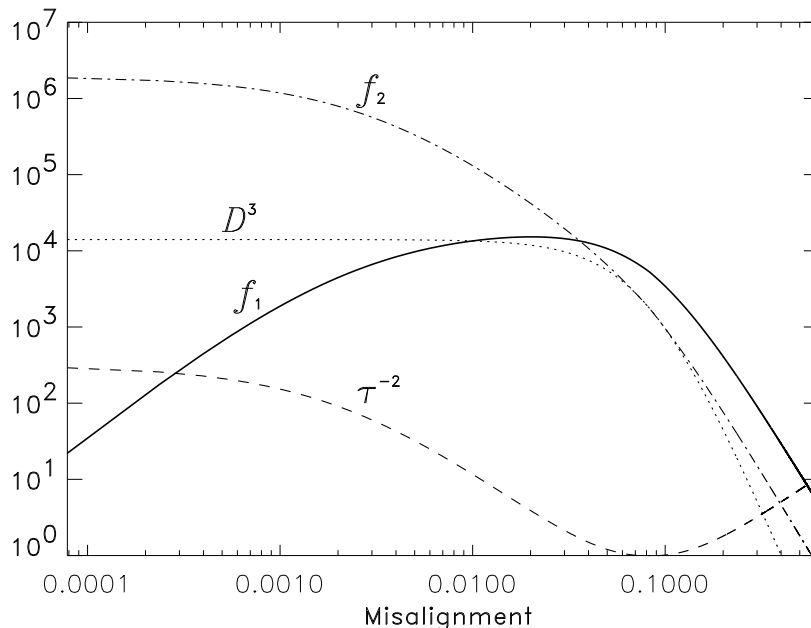


Figure 1: The square of the observable reduced timescale τ^{-2} (dashed) and the Doppler boost \mathcal{D}^3 (dotted) for the brightness temperature in case of intrinsic variations are shown together with the *flux-boosting factors* f_1 (solid) and f_2 (dash-dotted) as defined in the text. The misalignment is the angle θ between jet direction and line of sight. The assumed shock is travelling with $\Gamma_S = 6$ in a jet of $\Gamma_{\text{pre}} = 2.7$. The implied increase of observed T_b due to orientation changes f_1 is not substantially larger than \mathcal{D}^3 and the result of scanned perturbations f_2 is only sufficient for explaining IDV for strong alignment of jet and observer.

In Fig.1 the Doppler boosting of the flux due to intrinsic variations for a spherical source \mathcal{D}^3 is compared to the *flux-boosting factors* f_1 and f_2 for a shock with $\Gamma_S = 6$ in a jet with $\psi = 2.5^\circ$ and $\Gamma_{\text{pre}} = 2.7$ for the preshocked gas (resulting in a post shock gas with $\Gamma = 12$). Orientation changes of thin shocks require $\Delta\theta \sim \theta$ and consequently f_1 can not substantially increase the flux variations on short timescales compared to variability in a spherical source. Only if disturbances along the jet are highlighted by the passage of a shock can the flux variations be so rapid and strong that f_2 exceeds 10^6 which is necessary to bring a source with intrinsic $T_b \leq 10^{12}$ K up to the observed 10^{18} K. Nonetheless this cannot provide an explanation for most IDV sources, because it requires a misalignment of the line of sight to the jet direction much smaller than $1/(3\Gamma)$, where the plateau of \mathcal{D}^3 starts (see Fig.1). In the specific case shown in Fig.1 the misalignment must be less than $10^{-3}\Gamma^{-1}$, which cannot be reconciled with 25% of core-dominated sources showing IDV. Furthermore scanned perturbations in the jet

lead to variable optical depth in the shocked gas and timelags, which are not observed in cross correlations of IDV at different radio frequencies.

4 Refractive Interstellar Scintillation

It is known from pulsar measurements that compact radio sources are subject to scintillation in the ISM of our galaxy. Extragalactic sources flicker (Heeschen 1984) at frequencies $\nu \approx 1$ GHz with timescales of several days to weeks and this has been interpreted as a result of strong refractive scattering in the extended ISM of the galactic disk (Blandford, Narayan & Romani, 1986). The transition from strong to weak scattering is expected at about 5 GHz depending on the path length in the disk towards the source. The maximum of the modulation index m is ≈ 1 for a point source. A 1Jy source with an apparent T_b of 10^{12} K has a size of $230 \mu\text{as}$ at $\lambda 6\text{cm}$ and scintillation will be quenched¹, because the source size is much larger than the angular size of the Fresnel scale in the ISM. For a typical distance of 200 pc to the scattering medium, the expected modulation index is $m \leq 1.7\%$, while a source with $T_b = 10^{13}$ K will have $m \leq 5\%$ with a characteristic timescale of 0.5 days. Therefore any 1Jy source with apparent T_b above few $\times 10^{12}$ K is expected to scintillate with a timescale comparable to those observed in IDV sources, as has been demonstrated by Rickett et al. (1995) for 0917+624.

The light curves of scintillating sources contain further information, which can be explored via structure functions (SF) (Simonetti, Cordes & Heeschen, 1985):

$$\text{SF}(\tau) = \left\langle [\text{I}(t + \tau) - \text{I}(t)]^2 \right\rangle_t \quad . \quad (7)$$

The SF extracted from the data can be compared to theoretical expectations. For strong refractive and weak scintillation in an extended medium Coles et al. (1987) gave a closed form for SF's, which includes three cut-offs for the Fourier transform of the local SF. These are due to the Fresnel scale, the visibility amplitude, which contains the size of the source, and an exponential cut-off in strong scintillation giving rise to the refractive scale. Whichever comes first determines the modulation index and the slope of the SF below the first maximum (see Fig.2). Following Blandford, Narayan & Romani (1986) we assume a Gaussian distribution of ionized matter, keeping in mind that for IDV a much smaller scale height $H \sim 100\text{pc}$ is required than the ISM scale height in the galactic disk.

We concentrate on the modulation index derived from the plateau of the SF at large timelags and on the slope for shorter lags. It turns out that in weak scintillation the slope of the SF is either quadratic $\text{SF}(t) \propto t^\alpha$, $\alpha = 2$ for steep turbulent spectra $\beta \geq 4$ or $\alpha = \beta - 2$ for $\beta < 4$.

In strong and quenched scintillation the SF shows a broken power law below the maximum and this slope also depends on the power-law index β of the turbulent spectrum $\Phi(q) = C_N^2 q^{-\beta}$ of density fluctuations in the ISM. For the limiting case $\beta = 4$

¹A gaussian brightness distribution is assume for extended sources in this paper.

model	H [pc]	β	C_N^2 [$\text{m}^{-\beta-3}$]	θ_{S6} [μas]	θ_{S20} [mas]	v [km/s]
K	70	11/3	10^{-3}	40	0.4	5
S1	70	4.567	$10^{-10.6}$	40	0.16	14
S2	140	4.567	$10^{-12.15}$	40	0.16	30

Table 1: Parameters for the structure function models. The result for $\lambda 6\text{cm}$ and $\lambda 20\text{cm}$ are shown in Fig.2 and Fig.3. The angular size θ_{S6} and θ_{S20} are the source size at $\lambda 6\text{cm}$ and $\lambda 20\text{cm}$.

discussed in Blandford, Narayan & Romani (1986), this slope is $\alpha = 1$ in the quenched and strong case, while for a Kolmogorov-like spectrum $\beta = 11/3$ the slope is $\alpha = 5/6$ for strong scattering and $\alpha = 2/3$ for quenched scintillation. For quenched scintillation, the slope is generally $\alpha = \beta - 3$.

We have computed theoretical structure functions dominated by quenched scintillation and compared them to the observed data taken at $\lambda 20\text{cm}$ and $\lambda 6\text{cm}$ (Fig.2 and Fig.3). The parameters are the power-law index β , the strength of density fluctuations C_N^2 , the scale height H and the velocity of the observer relative to the ISM cloud. From simultaneous fitting of the SF's at 6 cm and 20 cm we can find plausible parameters and the size of source at these wavelengths. The model parameters are summarised in Table 1. It is clearly visible from Fig.2 and Fig.3 that a steep spectrum is preferred.

In particular the slope $\alpha \approx 1.3$ at $\lambda 20\text{cm}$ indicates a steep spectrum $\beta = 4.3$, when only quenched scintillation is assumed. The turbulent spectrum has to be even steeper because the SF flattens before turning over into the $\alpha = \beta - 2$ slope dictated by the Fresnel cut-off at smaller timelags. Together with the weak curvature near the plateau for large timelags, this points to the slope $\beta \approx 4.6$ of the models S1 and S2.

5 Conclusions

Based on IDV observations of several Quasar and BL Lac radio cores with apparent brightness temperatures in the range of 10^{16} – 10^{21} K we investigated the possibility of intrinsic variations due to the propagation of thin relativistic shocks. We find that no source with $T_b > 10^{16}$ K can be explained by that model without calling for Doppler factors larger than 20 and strong alignment between the jet and the line of sight. The required alignment firmly rules out this hypothesis as an explanation for all IDV sources.

Based on refractive interstellar scintillation IDV can be explained by turbulence in the ISM. The scale size of the ionized gas responsible for IDV is about 100 pc in the case of 0917+624, and scintillation is quenched by the source size, which is larger than the refractive or Fresnel scale in the ISM. A fit to the structure functions at $\lambda 20\text{cm}$ and $\lambda 6\text{cm}$ indicates a steep power law ($\beta \approx 4.6$) for $\Phi(q)$ fluctuations. This corresponds to an energy spectrum $\sim q^{-2.6}$ that is much steeper than both a Kolmogorov spectrum and the q^{-2} spectrum for compressible turbulence, but a bit shallower than

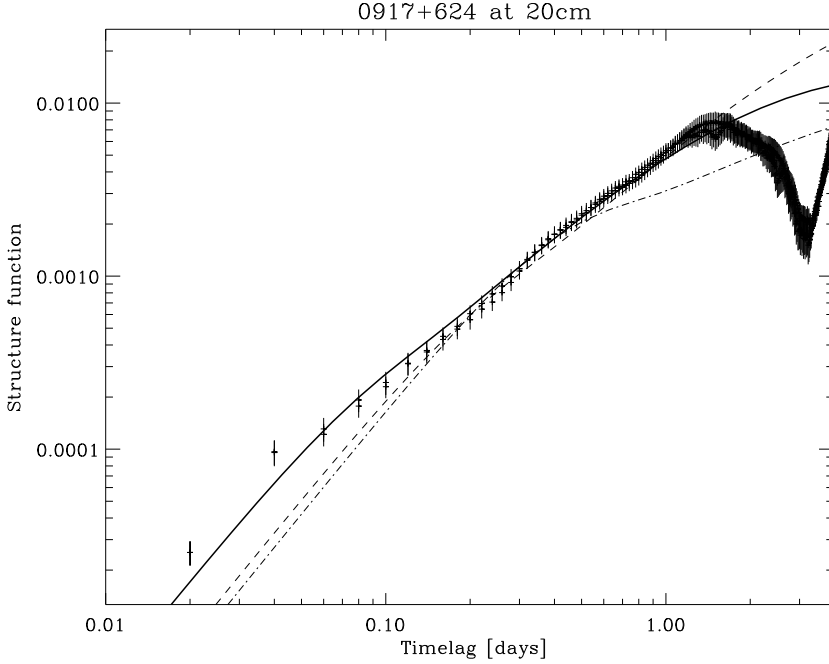


Figure 2: Structure function of total flux variations of 0917+624 at 20 cm in 1989. The data have recently been analysed by Qian et al. (2001). Over-plotted on the SF derived from the measurement are models for quenched scintillation according to Table 1. The dash-dotted line shows the model with a Kolmogorov spectrum (K). The step spectra models (S1 - dashed) and (S2 - solid) give better fits for the 20cm data.

$\sim q^{-3}$ expected for two-dimensional turbulence. The length scale probed in the ISM by these measurements are between $5 \cdot 10^8$ m and $2 \cdot 10^9$ m at the peak of the structure functions. The slope of the turbulent spectrum is derived from structure functions at small timelags and the corresponding spectrum extends an order of magnitude down to smaller spatial scales. Compressible turbulence is not unexpected at these scales, if turbulence is driven by shocks from supernovae or by stellar winds.

Scintillation in 0917+624 is quenched by the source size, which is one parameter of the theoretical fits to the SFs. The required sizes are $\sim 40 \mu\text{as}$ and $\sim 0.4 \text{ mas}$ at $\lambda 6\text{cm}$ and $\lambda 20\text{cm}$ respectively. At $\lambda 6\text{cm}$, the flux of 0917+624 (redshift $z = 1.446$) is 1.5 Jy . Combined with the derived source size this implies $T_b = 10^{14} \text{ K}$. Again Doppler factors of about 100 are needed to avoid the IC catastrophe or Doppler factors of 1000 to arrive at equipartition temperature. The sizes derived for 0917+624 from structure function models might be changed, if a degeneracy in the model parameters exists. The most plausible direction is an even closer ISM screen with a higher level of turbulence. In this case the angular Fresnel scale gets larger and larger source sizes are allowed.

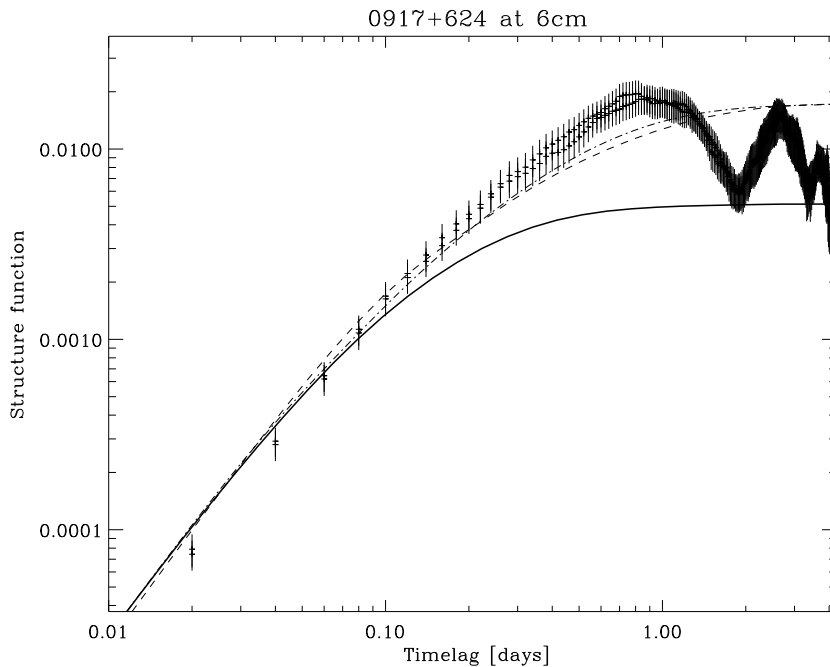


Figure 3: Structure function of total flux variations of 0917+624 at 6cm in 1997. The data come from one of the best sampled light curve at this wavelength. Over-plotted on the SF derived from the measurement are the same models for quenched scintillation like in Fig.2 applied to $\lambda 6\text{cm}$.

References

- Begelman, M.C., Rees, M.J., Sikora, M. 1994, *ApJ*, 429, L57
 Blandford, R., Narayan, R., Romani, R.W. 1986, *ApJ*, 301, L53
 Coles, W.A., Frehlich, R.G., Rickett, B.J., Codona, J. L. 1987, *ApJ*, 315, 666
 Heeschen D.S., 1984, *AJ* 89, 1111
 Heeschen D.S., Krichbaum T.P., Schalinski C.J., Witzel A., 1987, *AJ* 94, 1493
 Jones T.W., O'Dell S.L., 1977, *ApJ* 214, 522
 Qian S.J., Quirrenbach A., Witzel A., et al. 1991, *A&A*, 241, 15
 Quirrenbach A., Witzel A., Krichbaum T.P., et al., 1992, *A&A* 258, 279
 Readhead, A.C.S. 1994, *ApJ*, 426, 51
 Rickett, B.J., 1990, *ARA&A*, 28, 561
 Rickett, B.J., Quirrenbach, A., Wegner, R., Krichbaum, T.P., Witzel, A. 1995, *A&A*, 293, 479
 Simonetti J.H., Cordes J.M. Heeschen D.S., 1985, *ApJ* 296, 46
 Spada, M., Salvati, M., Pacini, F. 1999, *ApJ*, 511, 136
 Wagner S.J., Witzel A., 1995, *ARA&A* 33, 163